Engineered Science
DOI: https://dx.doi.org/10.30919/es1862

Comparative Analysis of Electron, Proton and Neutron Irradiation Damage in Gallium Arsenide Flexible Triple-Junction Solar Cells

Meng Li,[1,2] Abuduwayiti Aierken,[1,3,*] Tingbao Wang,[2] Shuyi Zhang,[2] Jinshun Bi,[1,3] Xuefei Liu,[1,3,*] Gang Wang,[1,3] Degui Wang,[1,3] Mingqiang Liu[1,3] and Changsong Gao[1,3]

Abstract

This paper presents a detailed investigation of the effects of 1 MeV electron, 1 MeV neutron, and 3 MeV proton irradiations on the performance of flexible inverted metamorphic GaInP/GaAs/InGaAs triple-junction (IMM3J) solar cells. The degradation mechanisms of the main electrical parameters and external quantum efficiency were quantitatively analyzed using an equivalent displacement damage dose (DDD) model. The experimental results demonstrate that significant performance degradation occurred after irradiation. When the DDD=3.82×10^{10} MeV/g, the maximum power output degraded to 82%, 74%, and 53% of its initial value under 1 MeV electron, 1 MeV neutron, and 3 MeV proton irradiation, respectively. External quantum efficiency degradation predominantly occurs in the long-wavelength region, with the InGaAs subcell exhibiting the most severe current density degradation under 3 MeV proton irradiation. Using the DDD model, the relative radiation damage coefficients for the IMM3J solar cells were determined to be R_{ep} = 3.04 (1 MeV electron to 3 MeV proton), and R_{np}=2.29 (1 MeV neutron to 3 MeV proton). Short circuit current and open circuit voltage degradation models were used to analyze the degradation mechanism of the IMM3J solar cells.

Keywords: IMM3J solar cell, Radiation effects, Irradiation damage, Degradation mechanism.
Received: 28 July 2024; Revised: 04 October 2025; Accepted: 21 October 2025
Article type: Research article.

1. Introduction

Multijunction GaAs-based solar cells have gained increasing significance in space-energy systems owing to their high conversion efficiencies. Conventional lattice-matched GaInP/GaAs/Ge triple-junction solar cells (LM3J) typically achieve an efficiency of approximately 30%; however, their performance is constrained by insufficient infrared spectrum utilization and current mismatch in the bottom subcell.[1] To meet the growing demand for high-efficiency space photovoltaics, recent research has focused on two primary approaches: developing novel bottom-cell materials with enhanced infrared absorption and designing multijunction architectures to optimize current matching and full-spectrum absorption. Furthermore, the challenges associated with lattice and thermal expansion coefficient mismatches in multijunction structures can be mitigated using advanced wafer bonding and buffer layer technologies.[2] Recent advancements in multijunction solar cell design have introduced novel architectures, including quantum dots and quantum wells, along with emerging materials such as InGaAs, GaInAsN, and GaInAsP. These developments provide promising pathways for the development of high-efficiency solar cells with enhanced spectral compatibility.[3,4] Among these innovations, inverted lattice-mismatched (IMM) GaInP/GaAs/InGaAs triple-junction solar cells have attracted significant research interest owing to their exceptional flexibility, high conversion efficiency, and light weight. This structure leverages $In_{1-x}Ga_xAs$ -based subcells and graded buffer layer technology to mitigate lattice mismatch effects.

A notable breakthrough was achieved by SHARP Corp., which successfully fabricated an IMM3J solar cell with a GaInP (1.88 eV)/GaAs (1.43 eV)/InGaAs (0.98 eV) configuration via structural optimization. The device demonstrated a remarkable conversion efficiency of 37.9% under standard AM1.5G illumination (1 sun) and 44.4% under concentrated light (302 suns, AM1.5D).[5] The IMM3J cells were fabricated using the inverted growth technology, wherein the epitaxial layers were initially deposited on the substrate before removal. This approach not only reduces the cell mass

[1]*School of Physics and Electronic Science, Guizhou Normal University, Guiyang, 550025, China*
[2]*School of Energy and Environment Science, Yunnan Normal University, Kunming, 650500, China*

substantially but also enhances the specific power of spacecraft solar arrays, which is a critical factor for lightweight space mission designs.[6] Compared with conventional rigid triple-junction GaAs solar cells, the IMM3J architecture incorporates a flexible substrate, significantly improving its packing efficiency while offering superior mechanical flexibility and adaptability for space applications.[7] Owing to these advantages, flexible IMM3J solar cells have become a key research focus for next-generation space photovoltaics. The operational performance of space solar cells is predominantly affected by charged particles (protons and electrons) and neutral particles (notably neutrons), all of which exhibit strong penetration capabilities in space radiation environments. These particles induce defect formation, which reduces the minority carrier lifetime and promotes the premature recombination of photogenerated electron–hole pairs, ultimately leading to performance degradation and compromising the long-term operational stability of spacecraft power systems.[5,8]

Understanding radiation damage mechanisms, performance degradation characteristics, and on-orbit behavior has become a critical research focus and prerequisite for new solar cell technologies to qualify for space applications. Therefore, comprehensive particle irradiation testing with varying fluences and energies is essential for simulating actual space conditions. Standard evaluation methodologies include current–voltage (I–V) characterization, dark current–voltage (DIV) analysis, external quantum efficiency (EQE) measurements, and photoluminescence (PL) spectroscopy.[7,9,10] These techniques enable a systematic investigation of the effects of electron, proton, and neutron irradiation on IMM3J solar cells, with particular attention paid to the degradation patterns in each subcell (GaInP, GaAs, and InGaAs) for radiation resistance assessment. While existing studies have primarily examined the effects of high-energy proton and electron irradiation, there remains a significant gap in systematic experimental data comparing electron, proton, and neutron irradiations under controlled conditions. This study addresses this research need by investigating the effects of 1 MeV electron, 3 MeV proton, and 1 MeV neutron irradiation on IMM3J solar cells. The analysis employs the displacement damage dose (DDD) equivalence model to quantify performance degradation and establish comparative damage coefficients across different radiation types and energies. This approach provides fundamental insights into cell degradation mechanisms under various space radiation conditions.

2. Experiments

The IMM3J GaInP/GaAs/InGaAs solar cells investigated in this study were fabricated using a low-pressure metal-organic chemical vapor deposition (LP-MOCVD, model Vecco k475i) system, grown on 4-inch GaAs substrates with a (100) orientation tilted by 15°±0.5° toward the (111)A plane. Trimethylaluminum (TMAl), trimethylgallium (TMGa), and trimethylindium (TMIn) were used as the group-III precursors, and high-purity AsH_3 and PH_3 were used as the group-V sources. Si_2H_6 and diethyltelluride (DETe) was used as the n-type dopant, while CCl_4 and trimethylzinc (DMZn) were used as the p-type dopant, respectively. The reactor pressure was set to 39 Torr, and the growth temperature ranged from 600 to 700 °C. More details of the epitaxial growth and sample fabrication processes have been reported in our previous work.[11] A critical feature of the device design was the implementation of a 4000 nm-thick graded buffer layer between the middle GaAs and bottom $In_{0.3}Ga_{0.7}As$ subcells, engineered to accommodate lattice mismatch while maintaining optimal current matching. All samples were grown to dimensions of 2 cm×4 cm. Fig. 1 illustrates the detailed device architecture of the IMM3J solar cells.

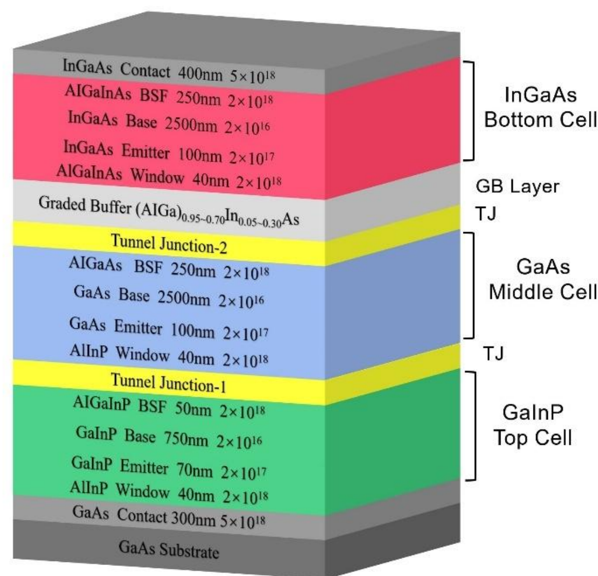

Fig. 1: Structure of the GaInP/GaAs/InGaAs (IMM3J) inverted lattice mismatched triple junction solar cell.

The 1 MeV electron and 3 MeV proton irradiation were conducted on an electron and proton accelerator, respectively, in a uniform flux (1.0×10^{11} e/cm^{2}s and 1.0×10^9 p/cm^{2}s) area at room temperature, at Space Environment Simulation Research Infrastructure (SESRI), Harbin Institute of Technology. The 1 MeV neutron irradiation was performed on the neutron reactor at China Academy of Engineering Physics, China, with a flux of 2.0×10^7 n/cm^{2}s. The proton and neutron fluences were calculated based on the DDD values determined by the non-ionizing energy loss (NIEL) method to guarantee consistency with the value of the DDD produced by the 1 MeV electron irradiation, while the electron fluences were chosen in accordance with the space solar cell evaluation and irradiation test standard.[12] The following equation was used to determine

[3]School of Integrated Circuits, Guizhou Normal University, Guiyang, 550025, China
*Email: erkin@gznu.edu.cn (Abuduwayiti Aierken); 201307129@gznu.edu.cn (Xuefei Liu)

the radiation induced DDD in solar cells[13]:

$$DDD = NIEL \times \varphi \quad (1)$$

where the φ is the irradiation fluence, NIEL is the non-ionizing energy loss value of solar cell materials for corresponding to the irradiation particles and its energy. The NIEL values of solar cell materials under irradiation were calculated by MULASSIS software.[14] Due to the very close NIEL values of GaInP, GaAs and InGaAs materials regarding to electron, proton and neutron irradiation,[15] $NIEL|_{1\ MeV\ electron}=3.82\times10^{-5}$ MeV·cm²/g, $NIEL|_{3\ MeV\ proton} = 2.25\times10^{-3}$ MeV·cm²/g and $NIEL|_{1\ MeV\ neutron} = 1.38\times10^{-2}$ MeV·cm²/g for IMM3J GaInP/GaAs/InGaAs solar cells have been applied for calculating DDD values in this work. The calculated irradiation fluences of the 3 MeV protons, 1 MeV neutrons, and selected 1 MeV electron fluences are shown in Table 1.

Table 1: The calculated irradiation fluences of 3 MeV protons and 1 MeV neutrons based on equivalent displacement damage (DDD) method.

1 MeV electron e/cm²	3 MeV proton p/cm²	1 MeV neutron n/cm²	*DDD* MeV/g
1.0×10^{14}	1.70×10^{11}	5.0×10^{11}	3.82×10^{9}
5.0×10^{14}	8.51×10^{11}	9.0×10^{11}	1.91×10^{10}
1.0×10^{15}	1.70×10^{12}	3.0×10^{12}	3.82×10^{10}

An OAI TSS-156 solar simulator was used to assess the I–V characteristics of the solar cells under standard AM0 spectra at T=25°C, before and after the irradiation. A SONF 7-SCSpec111 system was used to measure the external quantum efficiency (EQE) of the solar cells.

3. Results and discussion

3.1 Degradation of electrical properties

Fig. 2 presents the degradation behavior of the main electrical parameters of the IMM3J solar cells exposed to various particle radiations in terms of the short circuit current (I_{sc}), open circuit voltage (V_{oc}), maximum power (P_{max}), and fill factor (FF). The graph illustrates how irradiation with electrons, protons, and neutrons causes all the electrical characteristics of the solar cell to decrease monotonically as the DDD increases. There are notable variations in the degree of deterioration across several parameters, particularly the most significant parameter degradation caused by 3 MeV protons at the same DDD, despite the general electrical degradation trend of IMM3J solar cells being comparable. The P_{max} under irradiation with 1 MeV electrons, 1 MeV neutrons, and 3 MeV protons dropped to 84.84%, 79.40%, and 53.02% of the original values, respectively, for DDD = 3.82×10^{10} MeV/g.

According to reports on electron-irradiated Si and GaAs single-junction solar cells, the degradation rate V_{oc} is typically lower than that of I_{sc} when the irradiation fluences increased.[15-17] However, in this study, we observed that the degradation of V_{oc} was greater than that of I_{sc}, as shown in Fig. 2(a) and (b). The reason for this contrasting result is mainly the structure of the IMM3J solar cells, in which the overall output voltage of the solar cell is the sum of the V_{oc} of each subcell, whereas the output current is determined by the minimum current among the subcells. Therefore, the degradation of V_{oc} is faster than that of I_{sc} when the irradiation fluences increased. The primary reason for the degradation of

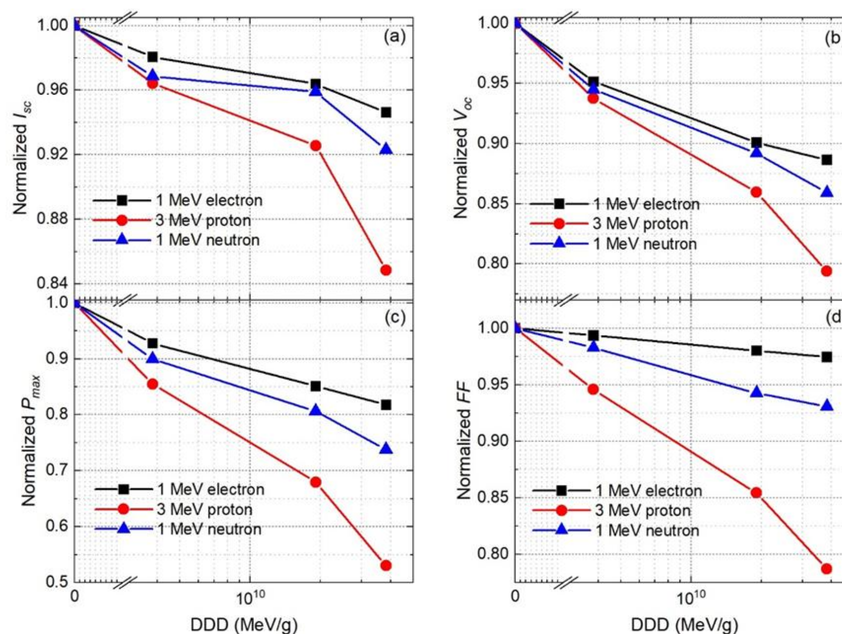

Fig. 2: Normalized values IMM3J solar cells before and after exposure to 1 MeV electrons, 3 MeV protons, and 1 MeV neutrons: (a) I_{sc}, (b) V_{oc}, (c) P_{max}, and (d) FF.

both V_{oc} and I_{sc} is the irradiation-induced lattice defects in the junction area, which act as nonradiative recombination centers and lead to a decrease in the minority carrier lifetime. Consequently, the degradation of V_{oc} and I_{sc} results in the degradation of $P_{\max}$ and FF (Fig. 2(c) and (d)).

In addition to directly obtaining the fundamental electrical parameters of the cell, the I–V curve allows the extraction of other parameters from the theoretical model, including the photogenerated current (I_{ph}), saturation current (I_0), diode ideal factor (n), parallel resistance (R_{sh}), and series resistance (R_s). The I–V curves of the IMM3J solar cells under 1 MeV electron, 3 MeV proton, and 1 MeV neutron irradiation are plotted in Fig. 3. The equivalent circuit model of a solar cell can be expressed as following equation[18,19]:

$$I = I_{ph} - I_0\left[\exp\left(\frac{V + IR_s}{nV_T}\right) - 1\right] - \frac{V + IR_s}{R_{sh}} \quad (2)$$

The extracted I_{ph}, I_0, n, R_{sh}, and R_s values from Fig. 3 obtained using Eq. (2) are listed in Table 2: The fitting results are in good agreement with the experimental data. This shows that under various irradiation particle types, I_0, n, and R_s all steadily increased with an increase in the DDD, whereas I_{ph} and R_{sh} exhibited a declining trend. Under 3 MeV proton irradiation, R_{sh} decreased by two orders of magnitude, which was more significant than that of electron and neutron irradiation. While the accumulation of lattice defects induced by irradiation in the non-junction region was mostly responsible for the increase in R_s, the decrease in $R_{sh,}$ is primarily ascribed to the increase in defect density in the p-n junction region. The electrical and optical performance of solar cells is affected by these displacement-damaged defects because they create new energy levels in the semiconductor energy bands, serve as nonradiative recombination centers, and decrease the collection efficiency of photogenerated minority carriers. The density of these displacement-damaged defects increases with an increase in the irradiation fluence and causes further degradation in the performance of the solar cell.

It has to be pointed out that the equivalent circuit model Eq. (2) is based on the single diode model, therefore, there must be some inaccuracies in the results listed in Table 2 due to the complex structure of a triple-junction solar cell with three junctions and two tunnel diodes in series. However, if we assume a triple-junction solar cell is equivalent as a single diode, the degradation trends of its electrical parameters may consistent with a single junction solar cell, and we can use these changes to qualitatively analyze the degradation behavior of the triple-junction solar cells as discussed above.

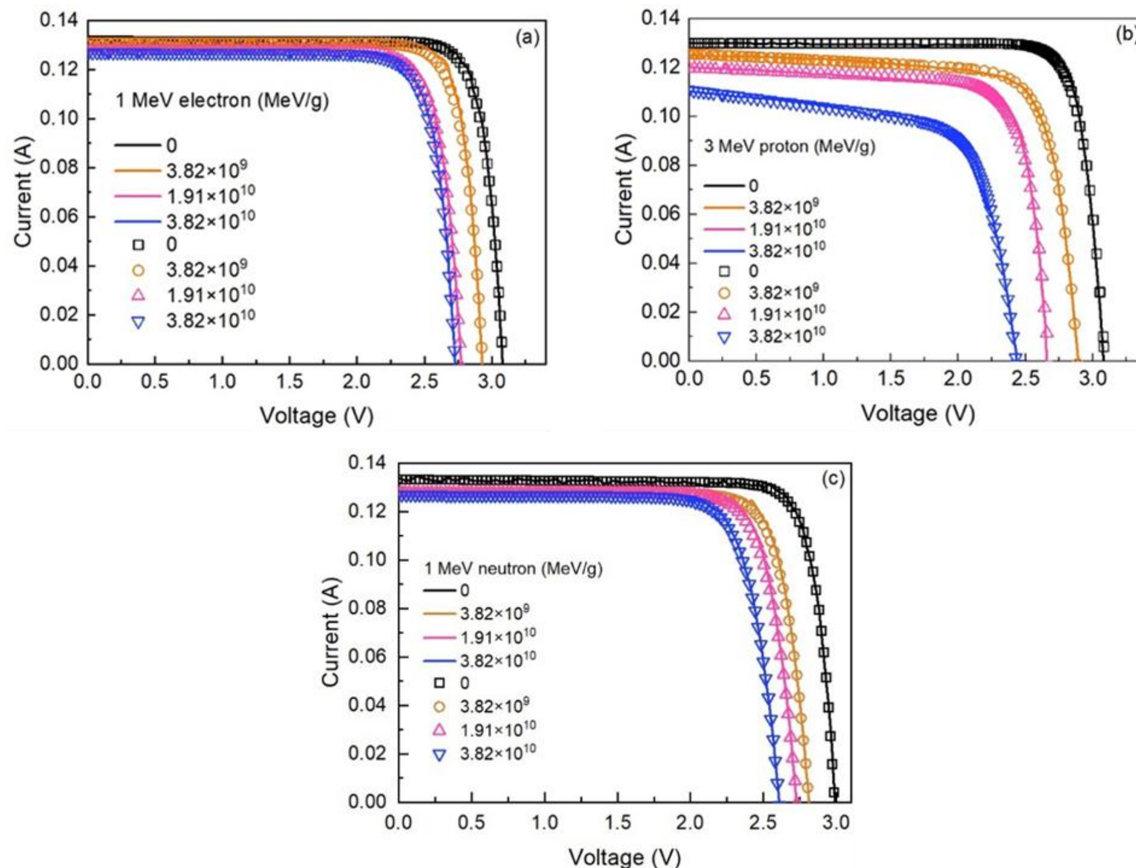

Fig. 3: Measured (lines) and fitted (symbols) I–V curves of IMM3J solar cells irradiated by (a) 1 MeV electrons, (b) 3 MeV protons, and (c) 1 MeV neutrons.

Table 2: I_{ph}, I_0, n, R_s and R_{sh} values extracted from Fig. 3.

	DDD (MeV/g)	I_{ph} (A)	I_0 (A)	n	R_s (Ω)	R_{sh} (Ω)
1 MeV electron	0	0.132	2.82×10^{-15}	3.76	0.128	15458
	3.82×10^{9}	0.131	1.12×10^{-14}	3.78	0.354	7824
	1.91×10^{10}	0.128	8.13×10^{-14}	3.8	0.411	7137
	3.82×10^{10}	0.127	4.28×10^{-12}	3.99	0.480	6858
3 MeV proton	0	0.131	2.50×10^{-15}	3.72	0.132	15503
	3.82×10^{9}	0.127	2.95×10^{-13}	3.85	0.420	4842
	1.91×10^{10}	0.124	1.15×10^{-12}	4.05	0.850	2842
	3.82×10^{10}	0.113	7.55×10^{-11}	4.48	1.250	971
1 MeV neutron	0	0.133	2.41×10^{-15}	3.73	0.130	15462
	3.82×10^{9}	0.128	8.66×10^{-14}	3.86	0.430	5500
	1.91×10^{10}	0.127	8.64×10^{-13}	3.99	0.443	5211
	3.82×10^{10}	0.127	6.43×10^{-12}	4.24	0.490	5006

3.2 Degradation of spectral response

The variation in the EQE values of IMM3J solar cells under electron, proton, and neutron irradiation at DDD = 3.82×10^{10} MeV/g is shown in Fig. 4. The degradation of the EQE is more pronounced in the long-wavelength region, particularly in the GaAs and InGaAs subcells, than in the short-wavelength region. Irradiation-induced defects and cell structure are the primary determinants of this phenomenon. High-energy electron, proton, and neutron irradiations generate significantly more defects in the base region of the cell than in the emitter region because of the difference in thickness of these two regions. Because the base region primarily absorbs long-wave photons, the probability of the photogenerated carriers, produced in the base region, being captured by irradiation-induced defects increases significantly, making the photon loss in the long-wavelength region more pronounced.[20] Furthermore, as direct bandgap semiconductors, GaAs and InGaAs exhibit a nonlinear connection between the photon energy and their optical absorption coefficients, which causes the short-wavelength photons to have a far shallower absorption depth than long-wavelength photons.[21] Hence, the possibility of electron-hole pairs being produced by short-wave photons captured by defects is much less.

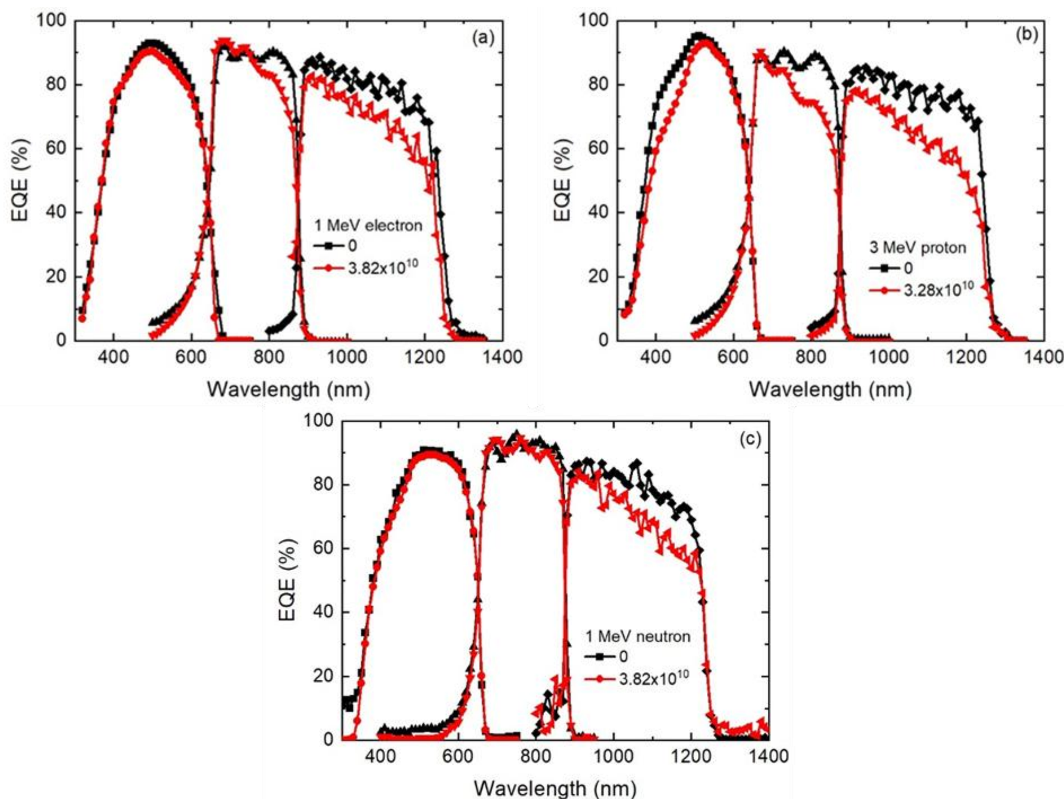

Fig. 4: EQE values of IMM3J solar cell under (a) 1 MeV electron, (b) 3 MeV proton and (c) 1 MeV neutron irradiation, DDD=3.82 × 10^{10} MeV/g.

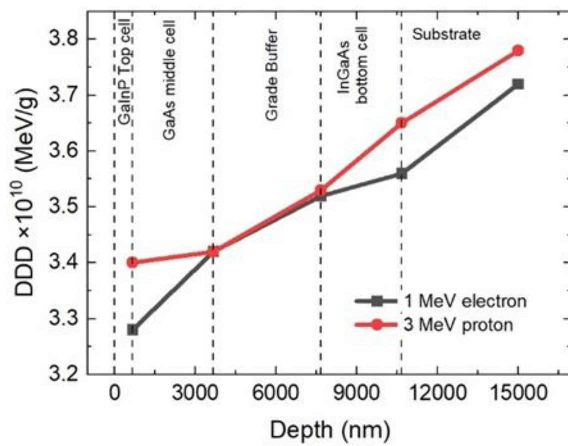

Fig. 5: DDD value of IMM3J solar cell.

The distribution of the DDD in each layer of the IMM3J solar cells with 1 MeV electron and 3 MeV proton irradiations was simulated using a multi-layer shielding simulation tool (MULASSIS),[22] as shown in Fig. 5. The simulation results show that independent of the particle type, the DDD increases with the depth of the incident irradiation particle from the top of the solar cell. This also supports the conclusion that irradiation induces more displacement damage in the base region than in the emitter region of the solar cell, resulting in severe degradation in the long-wavelength region.

The integrated current density (J_{sc}) of each subcell of the IMM3J solar cell can be obtained from Fig. 4 using the following equation[13]:

$$J_{sc} = \int_{\lambda_1}^{\lambda_2} \frac{q}{hc} \times EQE(\lambda) \times S(\lambda) \times \lambda \, d\lambda \qquad (3)$$

where S(λ) is the AM0 solar spectral intensity at λ. The extracted values of J_{sc} are listed in Table 3. The J_{sc} of the InGaAs subcell is the lowest compared to that of the GaInP and GaAs subcells before and after all electron, proton, and neutron irradiations, which indicates that the InGaAs subcell is the current-limiting subcell in the IMM-structured triple-junction solar cell. When DDD=3.82×10^{10} MeV/g, the remaining factors (RF) of J_{sc} of the InGaAs subcell are 0.944, 0.830, and0.912 for electron, proton, and neutron irradiations, respectively.

Irradiation introduces a certain amount of displacement damage to solar cell materials, and the particles lose energy on the front surface, junction area, and base area of the solar cell, resulting in a certain degree of degradation of the EQE over the entire absorption wavelength range. The relationship between I_{sc} and QE can be expressed by Eq. (4).[23]

$$I_{sc} = \sum qF(\lambda_i)[1 - R(\lambda_i)]QE(\lambda_i) \qquad (4)$$

From Eq. (4), I_{sc} is the integral of the quantum efficiency; therefore, the degradation of EQE will inevitably lead to a decrease in I_{sc}. In addition, displacement damage causes defects such as vacancies, interstitial atoms, and deep energy level centers in and near the junction area of the solar cell, which reduces the diffusion length and lifetime of carriers, causing an increase in the recombination and diffusion currents, that is, an increase in the dark current. It is known from Eq. (5)[24] that the output current is a linear superposition of the photocurrent and dark current; therefore, an increase in the dark current will lead to a decrease in the output current, causing a degradation in the electrical performance.

$$I(\lambda) = I_{dr} - (I_n + I_p) \qquad (5)$$

where I_{dr} is the photocurrent in the depletion region and I_n+I_p is the dark current. For a uniformly doped cell, V_{oc} is approximately equal to the built-in voltage V_D.[25] The value of V_D is related to the concentration of majority carriers. The introduction of irradiation defects into the cell creates the recombination center of the majority carriers, which reduces the concentration of majority carriers and thus leads to a decrease in V_{oc}.

From the results of the degradation of EQE curves, it can be seen that the GaInP top cell is affected the least among the three subcells under all irradiation conditions, this is mainly due to the stronger In-P bonds in GaInP.[26] Besides, from the material aspect, radiation resistance of GaInAs subcell is approximately equivalent to that of the InGaP and GaAs sub-cells.[7] However, during the growth of the step-graded buffer layer in IMM structure, it will introduce more crystal defects, such as threading dislocations,[27] in GaInAs bottom cell. After irradiation, these original defects will produce more displacement damages in solar cell active regions, and result in bigger degradation of cell performance.

3.3 Equivalent displacement damage dose modeling

To explore the correlation between different electron, neutron,

Table 3: Extracted integrated current density (J_{sc}) of the each subcell in the IMM3J solar cell.

	DDD	GaInP		GaAs		InGaAs	
	MeV/g	mA/cm^2	R.F.	mA/cm^2	R.F.	mA/cm^2	R.F.
1 MeV	0	17.13	1	17.08	1	16.87	1
electron	3.82×10^{10}	16.58	0.968	16.37	0.958	15.93	0.944
1 MeV	0	17.04	1	16.89	1	16.67	1
neutron	3.82×10^{10}	16.61	0.974	16.15	0.956	15.21	0.912
3 MeV	0	16.97	1	17.17	1	16.85	1
proton	3.82×10^{10}	15.88	0.935	15.20	0.885	13.99	0.830

Table 4: Fitting results for V_{oc}, I_{sc}, and P_{max} of IMM3J solar cells under electron, proton and neutron irradiations using Eq. (9).

Particle	Parameters	C	D_x (MeV/g)
1 MeV electron	I_{sc}	0.0420	7.54×10^9
	V_{oc}	0.0726	1.10×10^9
	P_{max}	0.1244	6.48×10^9
3 MeV proton	I_{sc}	0.1131	6.75×10^9
	V_{oc}	0.1999	2.39×10^9
	P_{max}	0.4443	2.13×10^9
1 MeV neutron	I_{sc}	0.0794	5.09×10^9
	V_{oc}	0.1129	4.69×10^9
	P_{max}	0.2188	4.87×10^9

and proton irradiation doses and the degradation of the solar cell performance, following a semi-empirical equation[18] was used to fit the results shown in Fig. 3.

$$\frac{P(D_d)}{P_0} = 1 - C\log\left(1 + \frac{D_d}{D_x}\right) \tag{6}$$

where D_d is the corresponding irradiation dose (DDD), C is the performance degradation rate, D_x is the critical DDD related to the cell structure, material, and irradiation particle energy, and P_0 and $P(D_d)$ are the electrical parameters of the solar cell before and after irradiation, respectively. The fitting results for V_{oc}, I_{sc}, and P_{max} of the IMM3J solar cell under 1 MeV electron, 3 MeV proton and 1 MeV neutron irradiations are listed in Table 4.

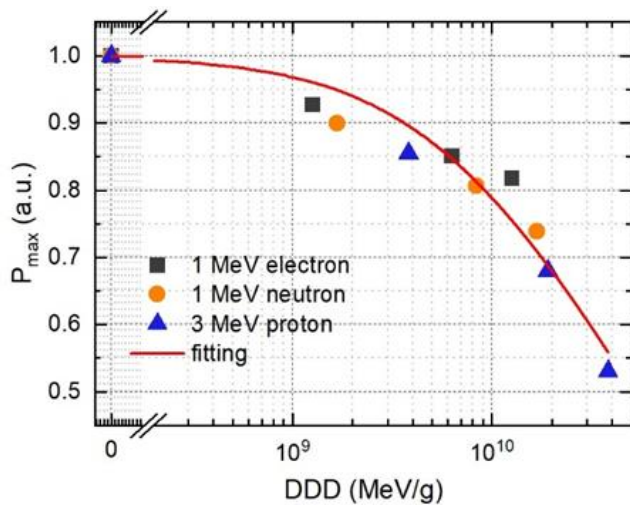

Fig. 6: Fitting results of P_{max} degradation curves of 1 MeV electron, 1 MeV neutron and 3 MeV proton irradiated IMM3J solar cells based on the equivalent damage model.

From the fitting results, it can be seen that the lattice-mismatched IMM3J solar cells have no obvious differences from traditional solar cells in terms of the irradiation damage effects on the output electrical performance. As shown in Table 4, the degradation rate (C) of P_{max} was the highest for all three types of irradiations. It is not difficult to understand that this is because the degradation of P_{max} is proportional to the degradation of I_{sc} and V_{oc}, and, when both I_{sc} and V_{oc}, are degraded, P_{max} has the highest degradation ratio. The electron–proton damage equivalent factor (R_{ep}) and the neutron–proton damage equivalent factor (R_{np}) are defined as $D_{\text{ex}}/D_{\text{px}}$ and $D_{\text{ex}}/D_{\text{nx}}$, respectively.[28] Based on the calculated R_{ep} =3.04 and R_{np} =2.29, the P_{max} degradation curves in Fig. 2(c) are re-plotted in Fig. 6.

The results show that the P_{max} degradation curves under electron and proton irradiations tended to overlap. Therefore, using the fitting parameters C, D_{x}, R_{ep} and R_{np}, the performance degradation of this type of solar cell under specific electron, proton and neutron irradiation conditions can be predicted. Furthermore, this method can be used to determine the proton fluence that causes the degradation of the solar cell parameters to be the same as that under the given electron irradiation conditions, and vice versa.

3.4 Short-circuit current degradation model and damage mechanism analysis

When high-energy particles interact with the solar cell, the lattice atoms deviate from their original positions, forming vacancies, and thereby generating defect centers in the semiconductor material. These defect centers act as traps for photogenerated electron–hole pairs, constituting displacement damage. Displacement damage is a cumulative damage process caused by high-energy incident particles through non-ionization energy loss. These defects can effectively shorten the diffusion length of minority carriers and reduce the collection efficiency of photogenerated electron–hole pairs, thereby leading to the degradation of solar cell performance.

For a single-junction solar cell, I_{sc} can be decomposed into the sum of the contributions of the n-type region current (I_{scn}), depletion region current (I_{scd}), and p-type region current (I_{scp}), that is $I_{\text{sc}} = I_{\text{scn}} + I_{\text{scd}} + I_{\text{scp}}$. By taking the derivative of each term in this equation, the expression for the total current density can be derived as[29]:

$$J_{sc} = \frac{q\alpha F(1-R)L}{e^{\alpha x_j}\alpha^2L^2-1}\left[\frac{\alpha L e^{-\alpha W_D}+\sinh\left(\frac{W_D}{L}\right)}{\cosh\left(\frac{W_D}{L}\right)} - \frac{\alpha L e^{\alpha x_j}-\sinh\left(\frac{x_j}{L}\right)}{\cosh\left(\frac{x_j}{L}\right)}\right] \tag{7}$$

where q is the electron charge number, α is the absorption coefficient, F is the incident light flux, R is the reflectivity, x_j is the depth of the p-n junction, W_D is the total thickness of the p-n junction, and L is the minority carrier diffusion length. In a typical III-V compound solar cell structure, α is approximately in the range of 10^4–10^5 cm^{-1}, x_j is a few hundred nanometers thick, and the thickness of the base layer is much greater than that of the emission layer ($W_D >> x_j$). Therefore, e^(-αW_D) ≈ e^(-αx_j) and sinh(W_D/L)≈cosh(W_D/L)≈cosh(x_j/L)≈1. So, Eq. (7) can be simplified as

$$J_{sc} = \frac{q\alpha F(1-R)L(1-\alpha L e^{\alpha x_j})}{e^{\alpha x_j}(\alpha^2 L^2 - 1)} = \frac{A\frac{1}{L} - \alpha A e^{\alpha x_j}}{\alpha^2 - \frac{1}{L^2}} \tag{8}$$

where $A = q\alpha F(1-R)\exp(-\alpha x_j)$. The degradation of the minority carrier diffusion length caused by charged particle irradiation can also be expressed as[30]

$$\frac{1}{L_\varphi^2} = \frac{1}{L_0^2} + K_L\varphi \tag{9}$$

where L_0 and L_φ are the minority carrier diffusion lengths of the solar cell before and after irradiation with different irradiation doses φ, and K_L is the diffusion length damage coefficient. Substituting Eq. (9) into Eq. (8), the relationship between the irradiation fluence and the current density of the solar cell is expressed as follows:

$$J_{sc} = \frac{\alpha A e^{\alpha x_j} - A(\frac{1}{L_0^2} + K_L\varphi)^{1/2}}{\frac{1}{L_0^2} - \alpha^2 + K_L\varphi} \tag{10}$$

When $\varphi = 0$, Eq. (10) becomes:

$$J_0 = \frac{\alpha A e^{\alpha x_j} - A/L_0}{\frac{1}{L_0^2} - \alpha^2} \tag{11}$$

The L_0 value of each subcell can be determined using J_0 values determined from the EQE (Table 3) and Eq. (11), and then, L_0 and the corresponding φ and J_{sc} of each subcell are substituted into Eq. (10) to calculate K_L. Tables 5 and 6 list the setting parameters and calculated values of L_0 and K_L for each subcell of the IMM3J solar cell under 1 MeV electron, 3 MeV proton, and 1 MeV neutron irradiations, respectively. The K_L value of the IMM3J solar cell irradiated by protons is higher than that of the cell irradiated by electrons, which also supports the result that the I_{sc} degradation of the IMM3J solar cell irradiated by protons is greater. As shown in Table 6, InGaAs has a slightly higher K_L value (one order of magnitude), which means that under the same irradiation fluence, the K_L degradation is more severe than that of the other two subcells. This result is consistent with the fact that the EQE value of the InGaAs subcell appears more degraded in Fig. 4.

Table 5: Selected parameters for Eq. (13).

	GaInP	GaAs	InGaAs
α (cm^{-1}) [31]	9.69×10^4	1.02×10^4	2.36×10^4
R (%) [32]	7.34	5.75	10.36
F (cm^{-2}s^{-1})[33]	1.14×10^{17}	0.95×10^{17}	0.89×10^{17}
x_j (cm)[13]	0.2×10^{-4}	0.2×10^{-4}	0.4×10^{-4}

Table 6: Calculated values of L_0 and K_L for the IMM3J subcells.

	GaInP	GaAs	InGaAs
L_0 (cm)	7.70×10^{-6}	9.28×10^{-5}	3.57×10^{-5}
K_L	1.11×10^{-9} (e) 9.97×10^{-8} (p) 1.60×10^{-8} (n)	3.56×10^{-9} (e) 5.53×10^{-7} (p) 5.20×10^{-8} (n)	1.45×10^{-8} (e) 3.73×10^{-6} (p) 6.23×10^{-11} (n)

According to the relationship and calculation results in Table 6, the change in the minority carrier diffusion length under different irradiation fluences can be obtained, and the results are shown in Fig. 7. It can be seen that the degradation rate of the minority carrier diffusion length (L) in the InGaAs subcell is the highest compared to the other two subcells for all three types of irradiations. This phenomenon is consistent with the fact that the InGaAs bottom subcell is the current-limiting unit of IMM3J solar cells.

The carrier diffusion length damage coefficient K_L reflects the degradation rate of the carrier diffusion length of the solar cells under irradiation. The irradiation damage mechanism also reflects the introduction rate of deep-energy-level defects, as shown in Eq. (12) and (13)[34]:

$$L^2 = D\tau \tag{12}$$

$$\tau^{-1} = \tau_0^{-1} + N_R\sigma\nu = \tau_0^{-1} + K_\varphi\nu\varphi \tag{13}$$

where τ_0 and τ are the minority carrier lifetimes before and

after irradiation; N_R is the concentration of non-radiative recombination centers; K_φ is the defect introduction rate; σ is the defect capture cross-section area; v is the minority carrier thermal velocity; and D is the minority carrier diffusion coefficient. Substituting Eq. (12) and (13) into Eq. (9), we obtain the relationship between the defect introduction rate and the diffusion length damage coefficient of solar cells under 1 MeV electron, 3 MeV proton, and 1 MeV neutron irradiations as following:

$$K_\varphi = \frac{D}{v} \times K_L \tag{14}$$

At a given ambient temperature, D and v of minority carriers remain constant and are not affected by the increase in irradiation fluence; D= 1.89×10^2 cm^2/s and 2.0×10^2 cm^2/s, and, v=4.84×10^5 m/s and 4.4×10^5 m/s, for InGaAs and GaAs, respectively.[35] Based on these parameters, the calculated values of K_φ for IMM3J subcells are listed in Table 7. The result shows that the defect introduction rate, K_φ, of InGaAs cells is significantly higher than that of GaAs and GaInP subcells, which is also the key factor for the rapid decline of I_{sc} in the InGaAs subcell. The defect introduction rate of subcells caused by proton irradiation is significantly higher than that caused by electron and neutron irradiation, further confirming that the radiation resistance of cells under proton irradiation is relatively weak.

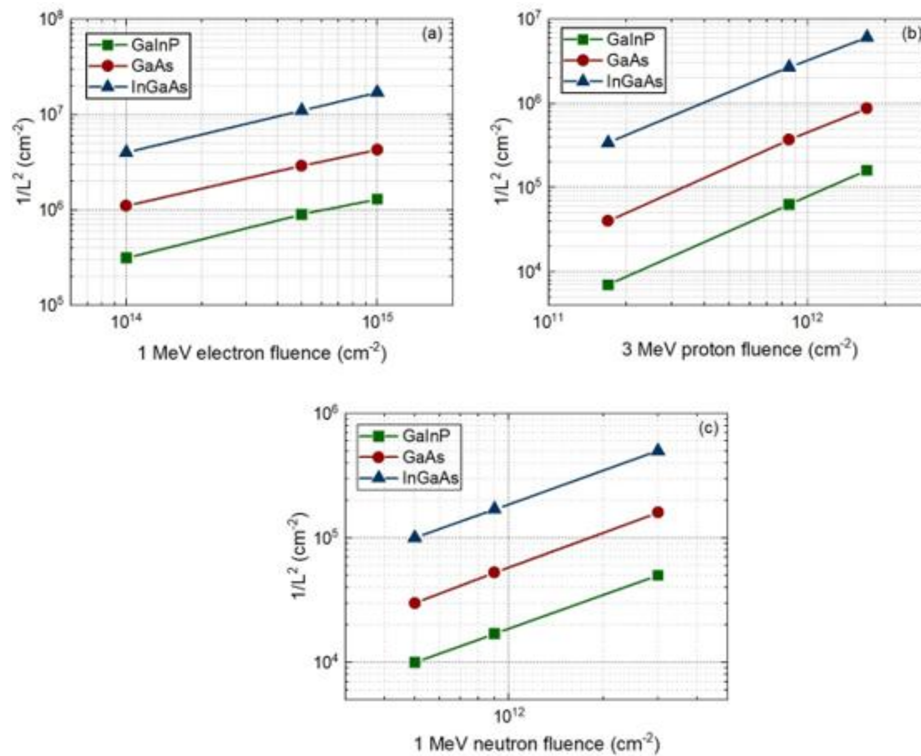

Fig. 7: Normalized 1/L^2 values after irradiation of (a) electrons, (b) protons and (c) neutrons in IMM cells with different irradiation injections.

Table 7: Calculated defect introduction rate of GaInP, GaAs, and InGaAs subcells exposed to 1 MeV electrons, 3 MeV protons, and 1 MeV neutrons irradiations.

	GaInP	GaAs	InGaAs
K_φ	2.78×10^{-13} (e) 2.49×10^{-11} (p) 4.00×10^{-12} (n)	1.62×10^{-12} (e) 2.51×10^{-10} (p) 2.36×10^{-11} (n)	5.65×10^{-12} (e) 1.45×10^{-9} (p) 6.23×10^{-11} (n)

3.5 Open-circuit voltage modeling and damage mechanism analysis

In a uniformly doped p-n junction solar cell, the open-circuit voltage can be approximated as its built-in electrical field, which is equivalent to the difference between the Fermi levels of p- and n-type semiconductors.[36] If the p-type semiconductor contains only acceptor impurities and the n-type contains only donor impurities, the built-in voltage of the p-n junction can be determined as follows:

$$V_D = \frac{k_B T}{q} \ln \frac{N_D N_A}{n_i^2} \tag{15}$$

where n_i is the intrinsic carrier concentration, T is the absolute temperature, k_B is Boltzmann's constant, q is the electron charge, N_A and N_D are the acceptor and donor concentrations, respectively. The doping concentration of the emitter and base

regions of solar cells is generally 10^{17}–10^{18} cm^{-3}. When all impurities are ionized, $N_D \approx n$, $N_A \approx p$, $n \approx p$, then[37]

$$V_D = \frac{k_B T}{q} \ln \frac{np}{n_i^2} = \frac{2k_B T}{q} \ln \frac{n}{n_i} \quad (16)$$

The concentration of displacement defects is positively correlated with the irradiation dose, whereas the carrier recombination rate caused by the defects is proportional to the defect concentration. Therefore, the presence of displacement defects reduces the concentration of majority carriers in semiconductor materials. Taking n-type semiconductors as examples, the majority carrier concentration after charged-particle irradiation can be expressed as[38,39]

$$n = n_0 - \varphi \frac{dn}{d\varphi} = n_0(1 - \alpha_n \varphi) \quad (17)$$

where n_0 and n are the majority carrier concentrations before and after irradiation, respectively; φ is the irradiation fluence. $K = dn/d\varphi$ is the majority carrier concentration removed per unit radiation dose, known as the carrier removal rate.[40] α_n is the damage coefficient related to the carrier removal rate, *i.e.*, $K = n_0\alpha_n$. During the irradiation process, the majority carrier concentration decreases continuously with increase in irradiation fluence, and the removal rate is approximately proportional to the majority carrier concentration,[41] *i.e.*, $K = n\alpha_n$

$$n = \frac{n_0}{1 + \alpha_n \varphi} \quad (18)$$

Substituting Eq. (18) into Eq. (16), we obtain the relationship between the built-in voltage and irradiation fluence as:

$$V_D = \frac{2k_B T}{q} ln \frac{n_0}{n_i(1 + \alpha_n \varphi)} = \frac{2k_B T}{q} [\ln \frac{n_0}{n_i} - \ln(1 + \alpha_n \varphi)] \quad (19)$$

Before irradiation, the irradiation fluence φ=0, then the built-in voltage before irradiation is

$$V_{D0} = \frac{2k_B T}{q} \ln \frac{n_0}{n_i} \quad (20)$$

Thus, the normalized built-in voltage is

$$\frac{V_D}{V_{D0}} = 1 - (\ln \frac{n_0}{n_i})^{-1} \ln{(1 + \alpha_n \varphi)} \quad (21)$$

Or

$$\frac{V_{oc}}{V_{oc0}} = \frac{V_D}{V_{D0}} = 1 - (\ln \frac{n_0}{n_i})^{-1} \ln{(1 + \alpha_n \varphi)} \quad (22)$$

Eq. (22) is consistent with the mathematical model of the solar cell electrical parameter degradation semiempirical equation (Eq. 6).

At room temperature, the intrinsic carrier concentrations n_i of the GaInP, GaAs and InGaAs subcells are 1.2×10^3 cm^{-3}, 1.79×10^6 cm^{-3} and 7.6×10^9 cm^{-3}, respectively, and the n_0 of each subcell is 1×10^{18} cm^{-3}.[42] Then, the degradation rates of V_{oc} for the GaInP, GaAs, and InGaAs subcells can be calculated using Eq. (22), which are 0.029, 0.037, and 0.053, respectively. This result further reveals that the InGaAs subcell degrades most significantly with an increase in the irradiation fluence.

4. Conclusion

We studied the electrical and optical properties of IMM3J solar cells grown using MOCVD and irradiated with 1 MeV electrons, 3 MeV protons, and 1 MeV neutrons. The results showed that the three irradiation methods caused serious degradation of the main electrical parameters and EQE values of the solar cells. Under the same DDD, proton irradiation caused more significant reductions in I_{sc}, V_{oc}, and P_{max} than electron and neutron irradiation. The spectral response was more severely degraded in the longer wavelength region of each subcell because the electron-hole pairs generated by longer wavelength photons near the band edge of the subcell farther from the junction interface suffer more post-irradiation collection degradation because of their sensitivity to the carrier diffusion length. When DDD=3.16×10^{10} MeV/g, the integrated current density J_{sc} of the InGaAs subcell degrades more under proton irradiation than under electron and neutron irradiations. The absolute values of Jsc of the GaInP and GaAs subcells before and after irradiation were lower than those of the InGaAs subcells, indicating that the InGaAs subcells were the current-limiting units in the solar cell structure.

The relative damage coefficients of the IMM3J solar cells irradiated with 1 MeV electrons to 3 MeV protons and 1 MeV neutrons to 3 MeV protons were determined by the DDD model, which are R_{ep}=3.04 and R_{np}=2.29, respectively. The modified solar cell performance degradation curves with the equivalent displacement damage dose model under electron, neutron, and proton irradiations almost overlap into a single line, and these relative damage coefficients can be used to evaluate the cell degradation performance under different energy particles. Based on the partitioned minority carrier collection model of the short-circuit current, the minority carrier diffusion length damage coefficient K_L and $1/L^2$ of each subcell under 1 MeV electron, 3 MeV proton and 1 MeV neutron irradiations were analyzed. The K_L of each subcell was higher under proton irradiation, and the diffusion length of the InGaAs subcell degraded the fastest, which is consistent with its current-limiting characteristics.

In addition, by calculating the defect introduction rate K_φ under different particle irradiations, it is found that the subcell K_φ caused by proton irradiation is significantly higher than that of electron and neutron irradiation, which further confirms that the radiation resistance of the solar cell under proton irradiation is relatively weak. Based on the open-circuit voltage degradation model, we calculated the degradation rate of each subcell's V_{oc}, revealing that the InGaAs subcell exhibited the most severe degradation with an increase in the

electron and proton irradiation fluence.

Acknowledgments
This work is supported by the National Natural Science Foundation of China (No. U2330121), Guizhou Provincial Scientists Workstation of Photovoltaic Materials and Devices (KXJZ[2024]031), Key Technology Innovation Talent Team for Micro-Nano Information Devices and Integrated Circuits in Guizhou Province (BQW[2024]014), Functional Materials and Devices Technology Innovation Team of Guizhou Province University (Qian Jiaoji [2023]058) and Guizhou Science and Technology Cooperation Platform SSYS [2025] Key Program No.005.

Conflict of Interest
The authors declare that they have no known competing financial interests or personal relationships that could have appeared to influence the work reported in this paper.

Supporting Information
Not applicable.

CRediT Statement
Meng Li: Writing - Original draft, Writing - Review & editing, Investigation, Methodology, Data curation, Software, Visualization, Formal analysis, Validation. **Abuduwayiti Aierken:** Conceptualization, Writing - original draft, Writing - Review & editing, Validation, Investigation, Methodology, Formal analysis, Resources, Supervision, Funding acquisition, Project administration. **Tingbao Wang:** Writing - Original draft, Writing - Review & editing, Investigation, Data curation, Software, Visualization, Formal analysis, Validation. **Shuyi Zhang:** Writing - Review & editing, Investigation, Data curation, Software, Visualization, Formal analysis, Validation; **Jinshun Bi:** Conceptualization, Validation, Formal analysis, Writing - Review & editing, Resources, Funding acquisition; **Xuefei Liu:** Conceptualization, Writing - Review & editing, Software, Validation, Methodology, Formal analysis, Resources, Supervision, Funding acquisition. **Gang Wang:** Writing - Review & editing, Data curation, Visualization, Formal analysis, Validation; **Degui Wang:** Writing - Review & editing, Data curation, Visualization, Formal analysis, Validation; **Mingqiang Liu:** Writing - Review & editing, Methodology, Software, Formal analysis, Validation. **Changsong Gao:** Writing - Review & editing, Data curation, Formal analysis, Validation.

References
[1] T. Sumita, M. Imaizumi, S. Matsuda, T. Ohshima, A. Ohi, H. Itoh, Proton radiation analysis of multi-junction space solar cells, *Nuclear Instruments and Methods in Physics Research Section B: Beam Interactions with Materials and Atoms*, 2003, **206**, 448-451, doi: 10.1016/s0168-583x(03)00791-2.
[2] F. Dimroth, M. Grave, P. Beutel, U. Fiedeler, C. Karcher, T. N. D. Tibbits, E. Oliva, G. Siefer, M. Schachtner, A. Wekkeli, A. W. Bett, R. Krause, M. Piccin, N. Blanc, C. Drazek, E. Guiot, B. Ghyselen, T. Salvetat, A. Tauzin, T. Signamarcheix, A. Dobrich, T. Hannappel, K. Schwarzburg, Wafer bonded four-junction GaInP/GaAs// GaInAsP/GaInAs concentrator solar cells with 44.7% efficiency, *Progress in Photovoltaics: Research and Applications*, 2014, **22**, 277-282, doi: 10.1002/pip.2475.
[3] F. Guffarth, R. Heitz, M. Geller, C. Kapteyn, H. Born, R. Sellin, A. Hoffmann, D. Bimberg, N. A. Sobolev, M. C. Carmo, Radiation hardness of InGaAs/GaAs quantum dots, *Applied Physics Letters*, 2003, **82**, 1941-1943, doi: 10.1063/1.1561165.
[4] P. N. K. Deenapanray, H. H. Tan, C. Jagadish, Influence of SiOx capping layer quality on impurity-free interdiffusion in GaAs/AlGaAs quantum wells, *MRS Online Proceedings Library*, 2000, **607**, 491, doi: 10.1557/PROC-607-491.
[5] T. Takamoto, H. Washio, H. Juso, Application of InGaP/GaAs/InGaAs triple junction solar cells to space use and concentrator photovoltaic, *IEEE 40th Photovoltaic Specialist Conference (PVSC)*, Denver, USA, June 8-13, 2014, 1-5, doi: 10.1109/PVSC.2014.6924936.
[6] J. Li, A. Aierken, Y. Liu, Y. Zhuang, X. Yang, J. H. Mo, R. K. Fan, Q. Y. Chen, S. Y. Zhang, Y. M. Huang, Q. Zhang, A brief review of high efficiency III-V solar cells for space application, *Frontiers in Physics*, 2021, **8**, 631925, doi: 10.3389/fphy.2020.631925.
[7] M. Imaizumi, T. Nakamura, T. Takamoto, T. Ohshima, M. Tajima, Radiation degradation characteristics of component subcells in inverted metamorphic triple-junction solar cells irradiated with electrons and protons, *Progress in Photovoltaics: Research and Applications*, 2017, **25**, 161-174, doi: 10.1002/pip.2840.
[8] K. Sasaki, T. Agui, K. Nakaido, N. Takahashi, R. Onitsuka, T. Takamoto, Development of InGaP/GaAs/InGaAs inverted triple junction concentrator solar cells, *9TH International Conference on Concentrator Photovoltaic Systems: CPV-9*, Miyazaki, Japan, 2013, 22-25, doi: 10.1063/1.4822190.
[9] J. Xu, K. Yang, Q. Xu, X. Zhu, X. Wang, M. Lu, Fabrication and irradiation effect of inverted metamorphic triple junction GaInP/GaAs/InGaAs solar cells, *Crystals*, 2022, **12**, 670, doi: 10.3390/cryst12050670.
[10] Y. Zhang, C. Qi, T. Wang, G. Ma, H.-S. Tsai, C. Liu, J. Zhou, Y. Wei, H. Li, L. Xiao, Y. Ma, D. Wang, C. Tang, J. Li, Z. Wu, M. Huo, Electron irradiation effects and defects analysis of the inverted metamorphic four-junction solar cells, *IEEE Journal of Photovoltaics*, 2020, **10**, 1712-1720, doi: 10.1109/JPHOTOV.2020.3025442.
[11] T. B. Wang, Z. X. Wang, S. Y. Zhang, M. Li, G. H. Tang, Y. Zhuang, X. Yang, A. Aierken, 1 MeV electron irradiation effect and damage mechanism analysis of flexible GaInP/GaAs/InGaAs solar cells, *Journal of Applied Physics*, 2024, **135**, 053103, doi: 10.1063/5.0184770.
[12] International Organization for Standardization (ISO), ISO 23038: 2018, Space systems space solar cells-electron and proton irradiation test methods, 2018.
[13] S. R. Messenger, E. M. Jackson, J. H. Warner, R. J. Walters, Scream: a new code for solar cell degradation prediction using

the displacement damage dose approach, *35th IEEE Photovoltaic Specialists Conference*, Honolulu, USA, June 20-25, 2010, 1106-1111, doi: 10.1109/PVSC.2010.5614713.

[14] C. Inguimbert, R. Gigante, NEMO: a code to compute NIEL of Protons, neutrons, electrons and heavy ions, *8th European Conference on Radiation and Its Effects on Components and Systems*, Cap d'Agde, France, September 19-23, 2005, PG2-1-PG2-8, doi: 10.1109/RADECS.2005.4365611.

[15] Messenger, Scott R., Edward A. Burke, Robert J. Walters, Jeffrey H. Warner, Geoffrey P. Summers, Justin R. Lorentzen, Thomas L. Morton, and Steven J. Taylor, Quantifying low energy proton damage in multijunction solar cells, *Proceedings of the 19th Space Photovoltaic Research and Technology Conference*, Ohio, USA, Feb 1, 2007.

[16] N. de Angelis, J. C. Bourgoin, T. Takamoto, A. Khan, M. Yamaguchi, Solar cell degradation by electron irradiation. Comparison between Si, GaAs and GaInP cells, *Solar Energy Materials and Solar Cells*, 2001, **66**, 495-500, doi: 10.1016/s0927-0248(00)00211-7.

[17] J. C. Bourgoin, M. Zazoui, Irradiation-induced degradation in solar cell: characterization of recombination centres, *Semiconductor Science and Technology*, 2002, **17**, 453-460, doi: 10.1088/0268-1242/17/5/308.

[18] J. Cubas, S. Pindado, M. Victoria, On the analytical approach for modeling photovoltaic systems behavior, *Journal of Power Sources*, 2014, **247**, 467-474, doi: 10.1016/j.jpowsour.2013.09.008.

[19] L. H. I. Lim, Z. Ye, J. Ye, D. Yang, H. Du, A linear method to extract diode model parameters of solar panels from a single I–V curve, *Renewable Energy*, 2015, **76**, 135-142, doi: 10.1016/j.renene.2014.11.018.

[20] Y. Zhang, Y. Wu, H. Zhao, C. Sun, J. Xiao, H. Geng, J. Xue, J. Lu, Y. Wang, Degradation behavior of electrical properties of inverted metamorphic tri-junction solar cells under 1 MeV electron irradiation, *Solar Energy Materials and Solar Cells*, 2016, **157**, 861-866, doi: 10.1016/j.solmat.2016.08.006.

[21] P. K. Sen, Nonlinear absorption in III: V semiconductors, *Physica Status Solidi (b)*, 1984, **124**, 117-125, doi: 10.1002/pssb.2221240113.

[22] F. Lei, R. R. Truscott, C. S. Dyer, B. Quaghebeur, D. Heynderickx, R. Nieminen, H. Evans, E. Daly, MULASSIS: a Geant4-based multilayered shielding simulation tool, *IEEE Transactions on Nuclear Science*, 2002, **49**, 2788-2793, doi: 10.1109/TNS.2002.805351.

[23] W. Ananda, External quantum efficiency measurement of solar cell, *15th International Conference on Quality in Research (QiR): International Symposium on Electrical and Computer Engineering*, Nusa Dua, Bali, Indonesia, July 24-27, 2017, 450-456, doi: 10.1109/QIR.2017.8168528.

[24] S. Zhao. Photo and dark current mechanisms in organic heterojunction solar cells, Stanford University ProQuest Dissertations & Theses, 2010, http:/purl.stanford.edu/qj736sk9775.

[25] T. Markvart, L. Castañer, Principles of solar cell operation, *McEvoy's Handbook of Photovoltaics*, Amsterdam, Elsevier, 2018, 3-28, doi: 10.1016/b978-0-12-809921-6.00001-x.

[26] N. Dharmarasu, M. Yamaguchi, A. Khan, T. Yamada, T. Tanabe, S. Takagishi, T. Takamoto, T. Ohshima, H. Itoh, M. Imaizumi, S. Matsuda, High-radiation-resistant InGaP, InGaAsP, and InGaAs solar cells for multijuction solar cells, *Applied Physics Letters*, 2001, **79**, 2399-2401, doi: 10.1063/1.1409270.

[27] A. Aierken, L. Fang, M. Heini, Q. M. Zhang, Z. H. Li, X. F. Zhao, M. Sailai, H. T. Liu, Q. Guo, W. Gao, H. Gao, Q. Sun, Effects of proton irradiation on upright metamorphic GaInP/GaInAs/Ge triple junction solar cells, *Solar Energy Materials and Solar Cells*, 2018, **185**, 36-44, doi: 10.1016/j.solmat.2018.04.035.

[28] S. R. Messenger, G. P. Summers, E. A. Burke, R. J. Walters, M. A. Xapsos, Modeling solar cell degradation in space: a comparison of the NRL displacement damage dose and the JPL equivalent fluence approaches, *Progress in Photovoltaics: Research and Applications*, 2001, **9**, 103-121, doi: 10.1002/pip.357.

[29] X. Gao, S.-S. Yang, Z.-Z. Feng, L. Zhang, Evaluation and prediction of the degradation of space Si solar cells induced by a low-earth-orbit radiation environment, *Chinese Physics C*, 2012, **36**, 900-904, doi: 10.1088/1674-1137/36/9/019.

[30] G. A. Umana-Membreno, J. M. Dell, T. P. Hessler, B. D. Nener, G. Parish, L. Faraone, U. K. Mishra, 60Co gamma-irradiation-induced defects in n-GaN, *Applied Physics Letters*, 2002, **80**, 4354-4356, doi: 10.1063/1.1483390.

[31] J. S. Cheong, A. N. A. P. Baharuddin, J. S. Ng, A. B. Krysa, J. P. R. David, Absorption coefficients in AlGaInP lattice-matched to GaAs, *Solar Energy Materials and Solar Cells*, 2017, **164**, 28-31, doi: 10.1016/j.solmat.2017.01.042.

[32] W.-J. Ho, Y.-Y. Lee, G.-C. Yang, C.-M. Chang, Optical and electrical characteristics of high-efficiency InGaP/InGaAs/Ge triple-junction solar cell incorporated with InGaAs/GaAs QD layers in the middle cell, *Progress in Photovoltaics: Research and Applications*, 2016, **24**, 551-559, doi: 10.1002/pip.2602.

[33] G. Oh, Y. Kim, S. J. Lee, E. K. Kim, Broadband antireflective coatings for high efficiency InGaP/GaAs/InGaAsP/InGaAs multi-junction solar cells, *Solar Energy Materials and Solar Cells*, 2020, **207**, 110359, doi: 10.1016/j.solmat.2019.110359.

[34] M. Sukeerthi, S. Kotamraju, Study of degradation in 3J inverted metamorphic (IMM) solar cell due to irradiation-induced deep level traps and threading dislocations using finite element analysis, *Physica E: Low-dimensional Systems and Nanostructures*, 2021, **127**, 114566, doi: 10.1016/j.physe.2020.114566.

[35] M. E. Levinshtein, S. L. Rumyantsev, Silicon (si), *Handbook Series on Semiconductor Parameters*, 1-32, doi: 10.1142/9789812832078_0001.

[36] K. O. Hara, N. Usami, Theory of open-circuit voltage and the driving force of charge separation in pn-junction solar cells, *Journal of Applied Physics*, 2013, **114**, 153101, doi: 10.1063/1.4825046.

[37] H. Amekura, N. Kishimoto, T. Saito, Photoconductivity evolution due to carrier trapping by defects in 17 MeV-proton irradiated silicon, *Journal of Applied Physics*, 1995, **77**, 4984-

4992, doi: 10.1063/1.359307.
[38] A. F. Behle, R. Zuleeg, Fast neutron tolerance of GaAs JFET's operating in the hot electron range, *IEEE Transactions on Electron Devices*, 1972, **19**, 993-995, doi: 10.1109/T-ED.1972.17532.
[39] M. Yamaguchi, S. J. Taylor, S. Matsuda, O. Kawasaki, K. Ando, Analysis of damage to silicon solar cells by high fluence electron irradiation, *Conference Record of the Twenty Fifth IEEE Photovoltaic Specialists Conference*, Washington DC, USA, May 13-17, 1996, 167-170, doi: 10.1109/PVSC.1996.563973.
[40] H. J. Stein, R. Gereth, Introduction rates of electrically active defects in *n*- and *p*-type silicon by electron and neutron irradiation, *Journal of Applied Physics*, 1968, **39**, 2890-2904, doi: 10.1063/1.1656690.
[41] C.-H. Lin, C. W. Liu, Metal-insulator-semiconductor photodetectors, *Sensors*, 2010, **10**, 8797-8826, doi: 10.3390/s101008797.
[42] S.-I. Sato, H. Miyamoto, M. Imaizumi, K. Shimazaki, C. Morioka, K. Kawano, T. Ohshima, Degradation modeling of InGaP/GaAs/Ge triple-junction solar cells irradiated with various-energy protons, *Solar Energy Materials and Solar Cells*, 2009, **93**, 768-773, doi: 10.1016/j.solmat.2008.09.044.

Publisher's Note: Engineered Science Publisher remains neutral with regard to jurisdictional claims in published maps and institutional affiliations.

Open Access
This article is licensed under a Creative Commons Attribution-NonCommercial-NoDerivatives 4.0 International, which permits the use, sharing, adaptation, distribution and reproduction in any medium or format, as long as appropriate credit to the original author(s) and the source is given by providing a link to the Creative Commons license. This usage for commercial purposes is not allowed. If modifications, adaptations or any other transformation were made, it is not allowed for distribution. The images or other third-party material in this article are included in the article's Creative Commons license, unless indicated otherwise in a credit line to the material. If material is not included in the article's Creative Commons license and your intended use is not permitted by statutory regulation or exceeds the permitted use, you will need to obtain permission directly from the copyright holder. To view a copy of this license, visit https://creativecommons.org/licenses/by-nc-nd/4.0/.

©The Author(s) 2025.